Supplementary Materials for

Conflicts in natural selection constrain adaptation to climate change in *Arabidopsis thaliana*

Megan Ruffley*, Laura Leventhal, Shannon Hateley, Seung Y. Rhee, Moises Exposito-Alonso*

*corresponding author: meganrruffley@gmail.com

This PDF file includes:

Tables S1 to S20
Figs. S1 to S24

Supplemental Tables

SupplementalTables_Ruffleyetal2023.xls

Table S1 Phenotypes gathered for this study with the original publication, general name of the phenotype, number of 1001 genomes accessions used in the original study, general function category, and stress strategy classification.

Table S2 Imputation accuracy (NRMSE) for each phenotype.

Table S3 Phenotype-phenotype Pearson correlation coefficients that are significant between flowering time, WUE, and growth rate phenotypes associated with all other phenotypes. NAs indicate there were not enough overlapping samples to perform an estimate of the correlation.

Table S4 Pearson's correlation coefficient between the target 64 phenotypes relating to drought and latitude for the 515 focal accessions.

Table S5 Pearson's correlation coefficient for select phenotypes, latitude, and longitude associated with bioclimatic, temperature, precipitation, evapotranspiration rate estimates, and genetic PC variables.

Table S6 Total selection coefficients measured for 1823 traits and 20 PC axes. using 3 fitness traits measured across two environments (Tubingen and Madrid; t/m), two rainfall treatments (high and low; h/l) and two planting densities (individual and population; i/p).

Table S7 Total selection coefficients measured for PC axes 1 and 2 with all fitness traits, measured across two environments (Tubingen and Madrid; t/m), two rainfall treatments (high and low; h/l) and two planting densities (individual and population; i/p).

Table S8 Total selection coefficients measured for flowering time traits from Exposito-Alonso et al. (2019) with 3 fitness traits, measured across two environments (Tubingen and Madrid; t/m), two rainfall treatments (high and low; h/l) and two planting densities (individual and population; i/p).

Table S9 Significant total selection coefficients measured for flowering time traits from various other studies associated with 3 fitness traits from Exposito-Alonso et al 2019, measured across two environments (Tubingen and Madrid; t/m), two rainfall treatments (high and low; h/l) and two planting densities (individual and population; i/p).

Table S10 Significant total selection coefficients measured for growth rate related traits associated with 3 fitness traits measured across two environments (Tubingen and Madrid; t/m), two rainfall treatments (high and low; h/l) and two planting densities (individual and population; i/p).

Table S11 Significant total selection coefficients measured for primary and secondary dormancy related traits associated with 3 fitness traits measured across two environments (Tubingen and Madrid; t/m), two rainfall treatments (high and low; h/l) and two planting densities (individual and population; i/p).

Table S12 Total selection coefficients measured for Delta_C13 associated with 3 fitness traits measured across two environments (Tubingen and Madrid; t/m), two rainfall treatments (high and low; h/l) and two planting densities (individual and population; i/p).

Table S13 Phenotype sample overlap with corresponding accession fitness data; numbers indicate the total number of individuals with raw phenotype data for the same individuals with fitness data. Fitness data also includes data from Fournier-Level et al. 2011 and Manzano-Piedras et al. 2014.

Table S14 Direct and total selection estimates from the dry-hot environment (Madrid, low water) for both planting densities (individual/population; i/p).

Table S15 Direct and total selection estimates from the cool-wet environment (Tubingen, high water) for both planting densities (individual/population; i/p).

Table S16 Summary heritability estimates and parameters from GWA of 12 target phenotypes; number of samples with data for a given phenotype, h estimate from BSLMM (not this is a hyperparameter and not heritability estimate exactly), PVE or proportion of variation explained from BSLMM (this IS the heritability estimate from BSLMM), rho is a hyperparameter on the polygenicity of a given trait, PGE is the proportion of genetic variance explained by sparse effect terms (~major effect loci), pi is the proportion of SNPs with non-zero effects, N gamma is the estimated number of loci with large effects, pve_norm is the SNP-based heritability estimate from the GWA run with normalized data, and pve_raw is the SNP-based heritability estimate from the GWA run with raw data.

Table S17 Selection response predictions (Z) for the cool-wet environment (Tubingen, high water) and the hot-dry environment (Madrid, Low water), for both planting densities (individual/population; i/p).

Table S18 Curated GO annotations for FT and dC13 multivariate GWA top hits.

Table S19 Curated GO annotations for FT and dC13 multivariate GWA using 5 genetic PCs top hits.

Table S20 Curated GO annotations for FT and dC13 imputed multivariate GWA top hits.

Table S21 Curated GO annotations for FT and dC13 imputed multivariate GWA using 5 genetic PCs top hits.

Supplemental Figures

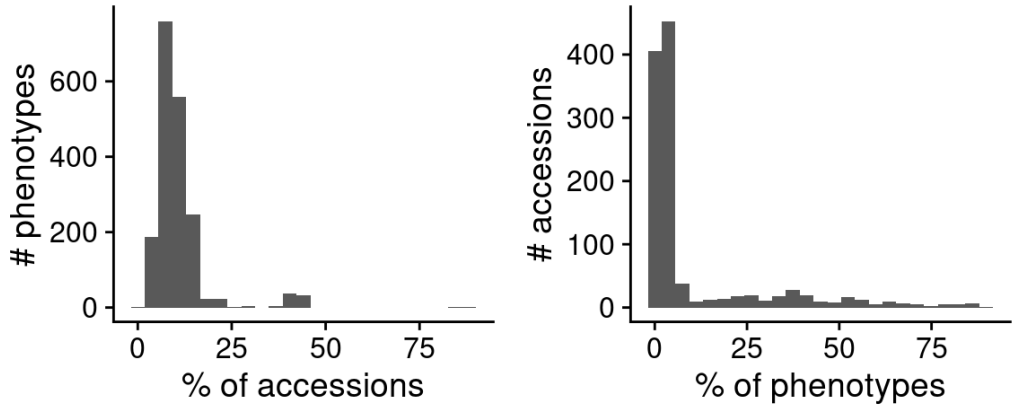

Figure S1. Trait coverage or missing trait data across the 1001 Genomes *A. thaliana* Accessions (**left**) and the traits (**right**).

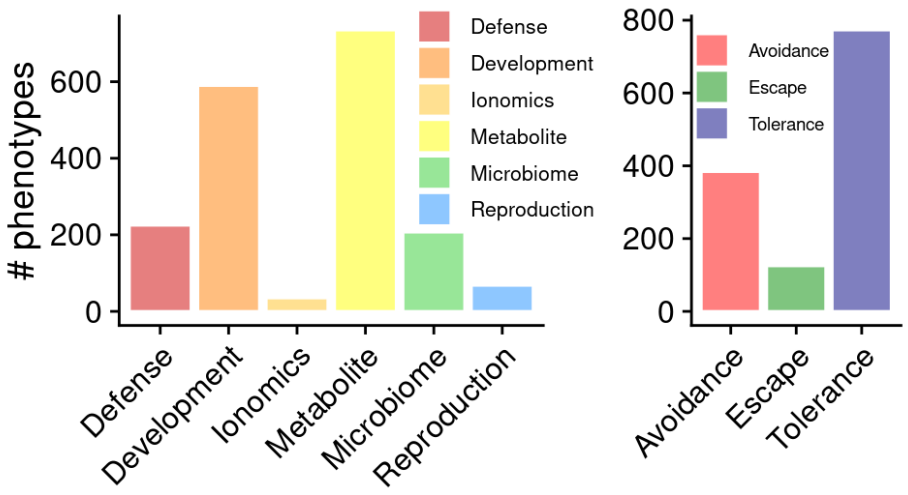

Figure S2. Raw counts of traits classified into general phenotype categories (**left**) and drought response strategies (**right**).

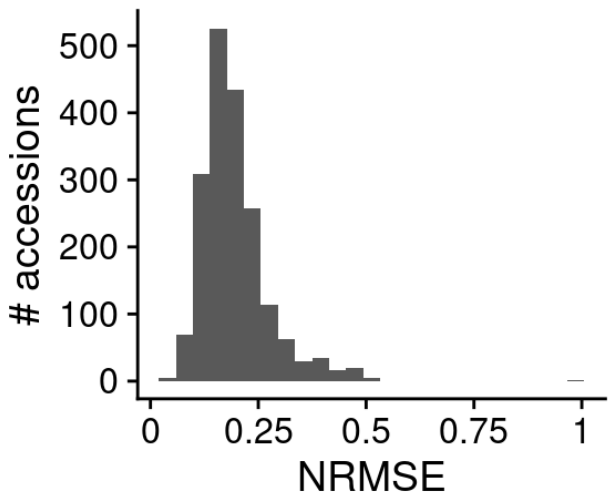

Figure S3. Histogram of Normalized root-MSE for all phenotypes in the imputation dataset.

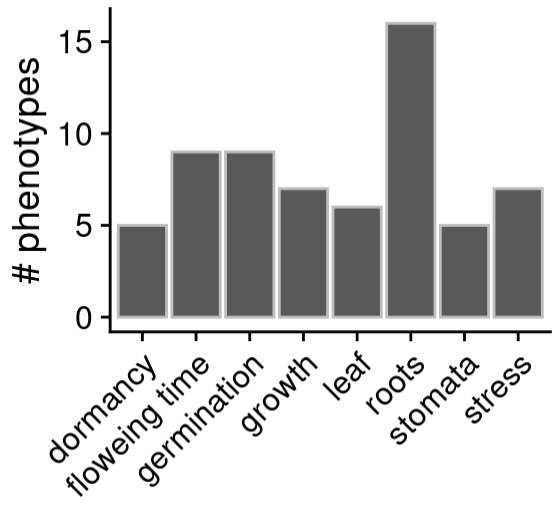

Figure S4. Counts of 64 traits in different functional trait categories used in the principle components analysis of Fig. 1A and Fig. S5.

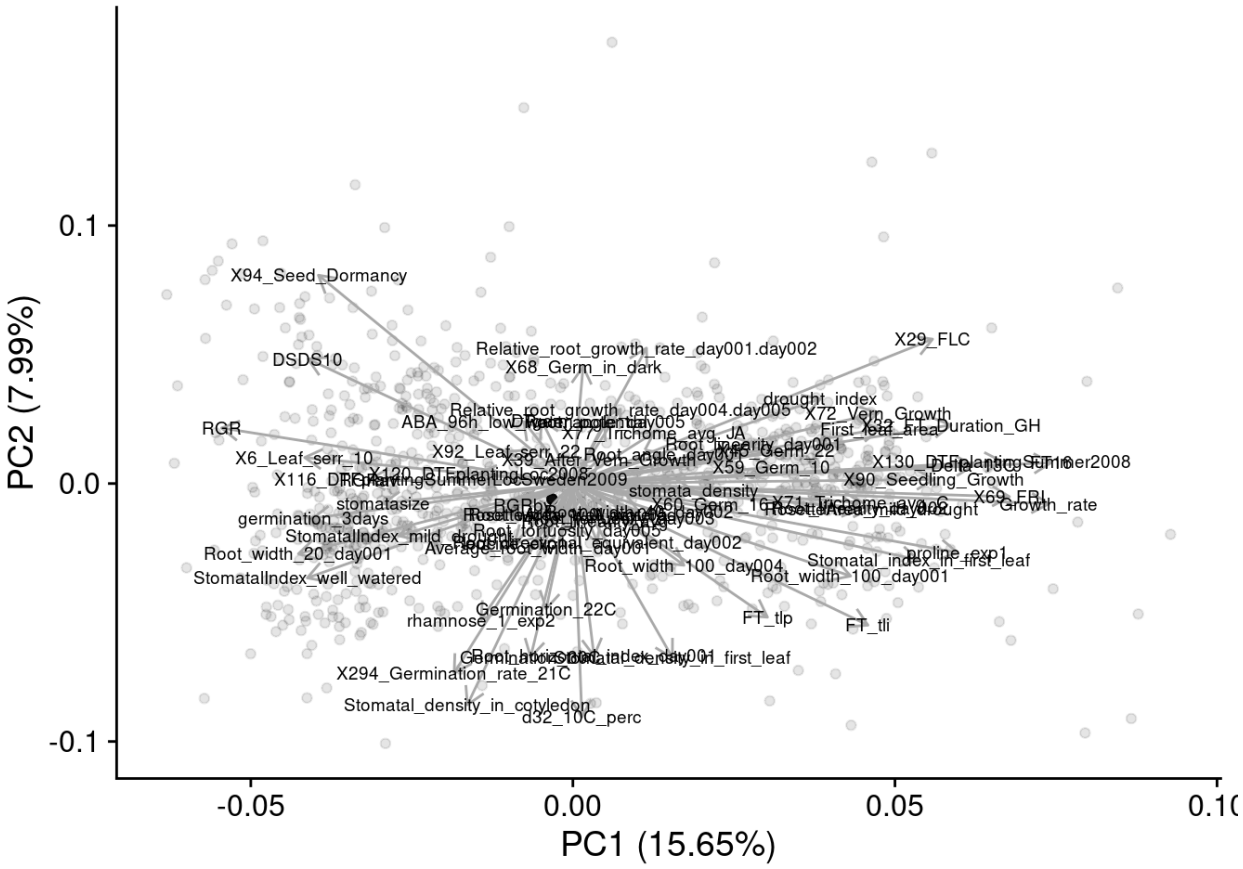

Figure S5. PCA axes 1 (15.6%) and 2 (7.9%) of 64 target phenotypes for all Eurasian accessions of *A. thaliana* (n=999); trait associations are in the same direction as in Fig. 1A.

.

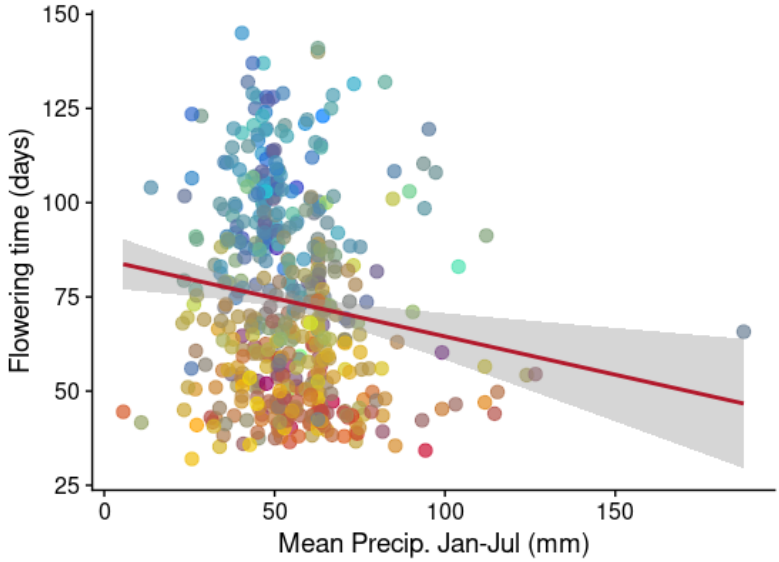

Figure S6. Correlation between mean precipitation Jan-July in Eurasia range locations and flowering time. R^2 = -0.14, p-value = 0.002. In a model of flowering time ~ annual precipitation + latitude + 4 genetic pcs, the coefficient for mean precipitation was estimated to be -0.122, p-value = 0.081.

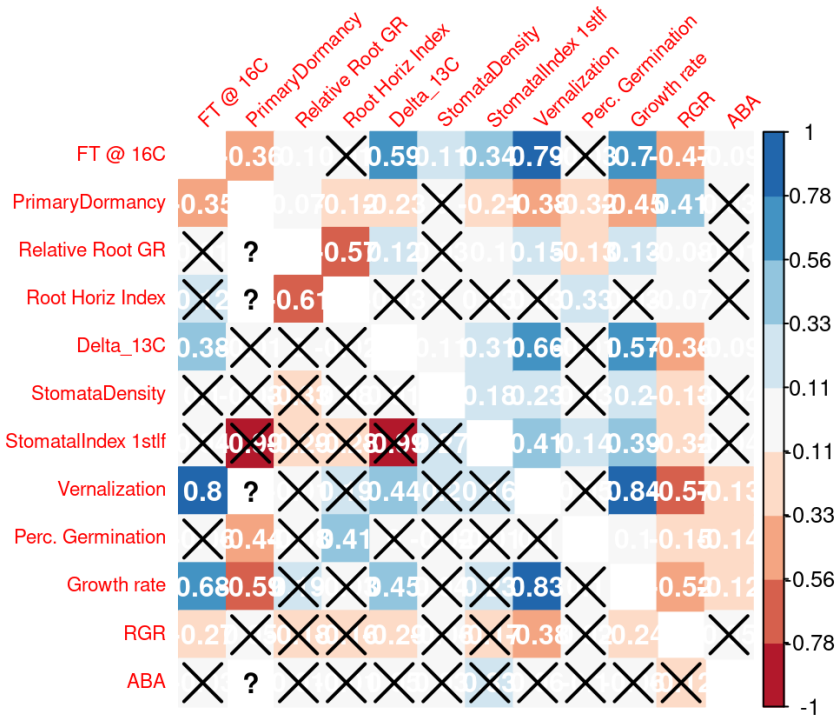

Figure S7. Pearson's correlation coefficients for 12 target phenotypes used in multivariate selection analysis. Upper right triangle are the correlations of imputed phenotype data and the lower left triangle are the correlations of raw data, and X indicates the correlation was not significant (p-value > 0.05).

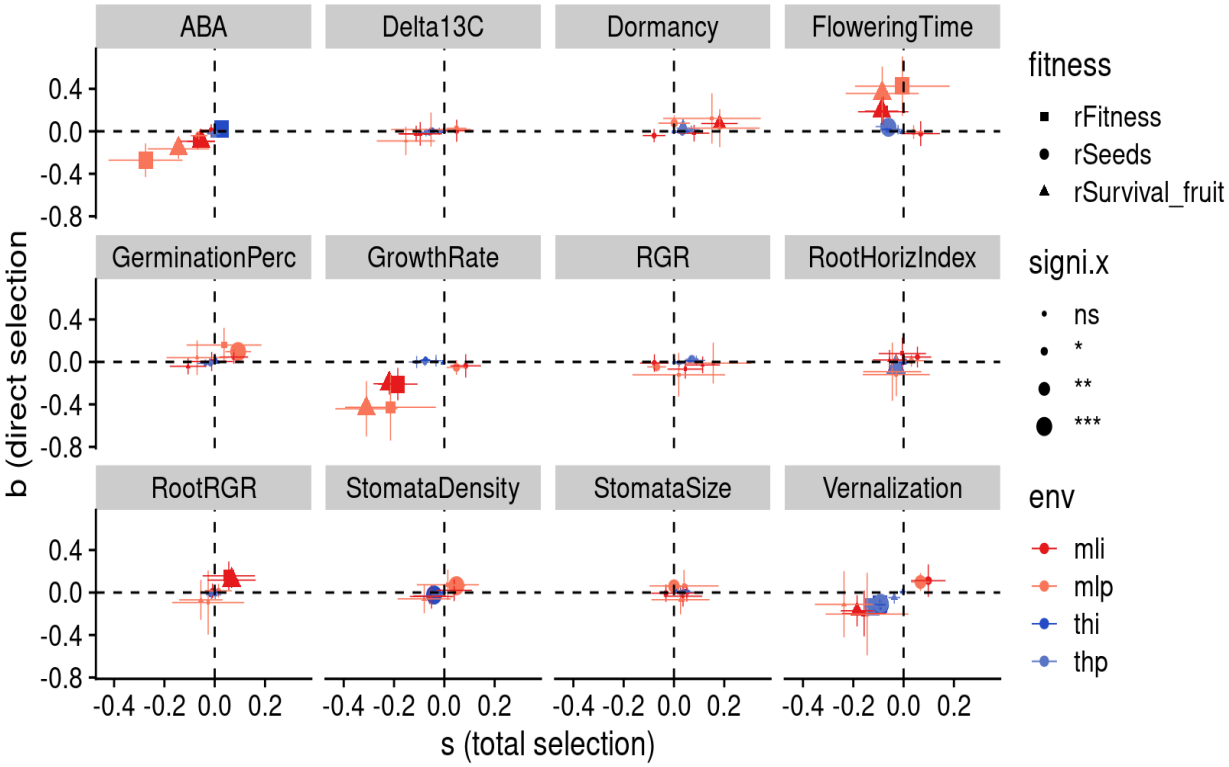

Figure S8. Multivariate selection analysis for 12 focal traits with dry and hot, cool and wet, and high/low planting density fitness data from Exposito-Alonso et al. 2019. Estimates were made from 100 bootstrap samples, establishing the confidence intervals and significance levels; ns= not significant, *=0.05, **=0.01, ***=0.001.

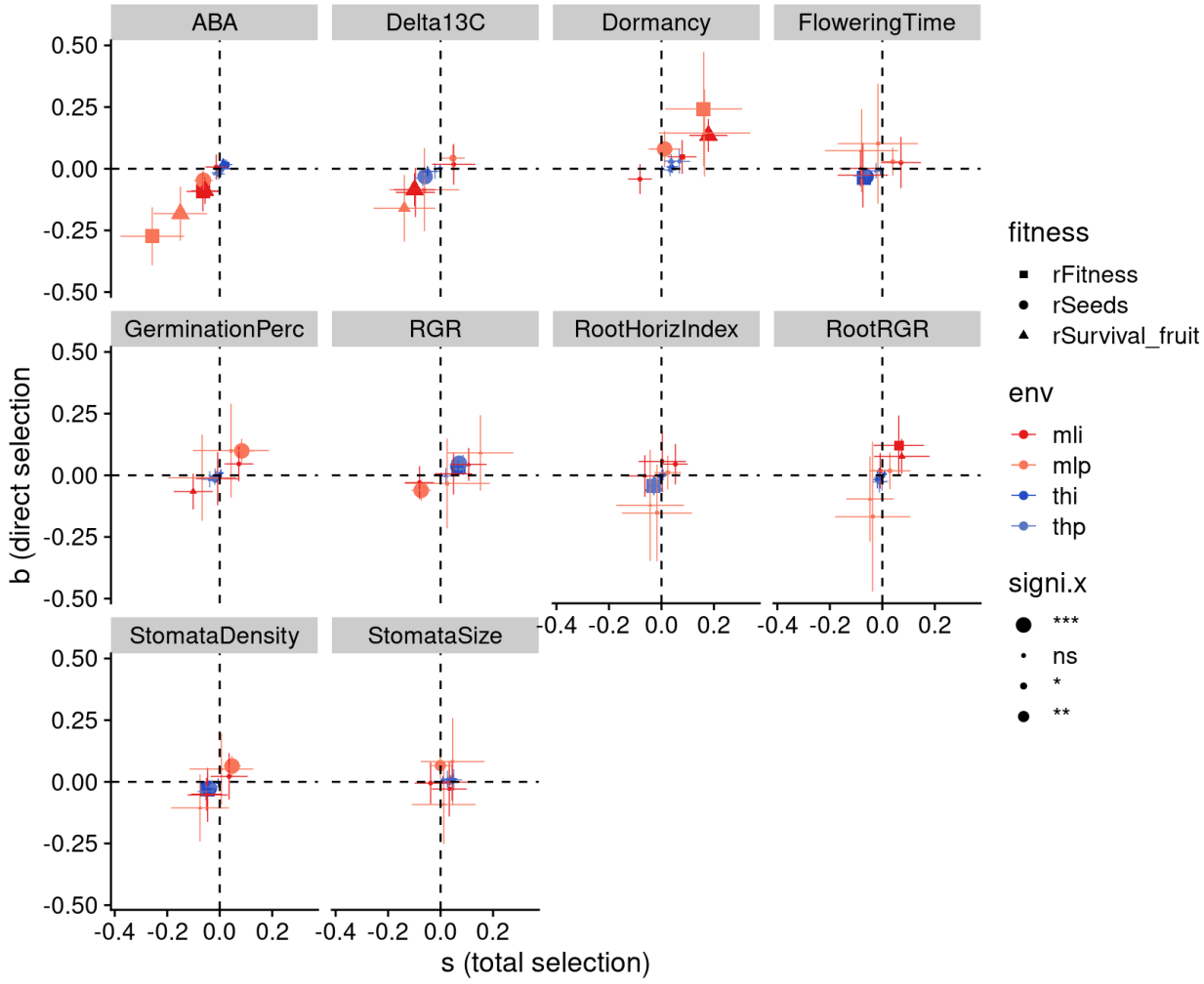

Figure S9. Multivariate selection analysis for 10 focal traits (growth rate and vernalization growth removed) with dry and hot, cool and wet, and high/low planting density fitness data from Exposito-Alonso et al. 2019. Estimates were made from 100 bootstrap samples, establishing the confidence intervals and significance levels; ns= not significant, *=0.05, **=0.01, ***=0.001.

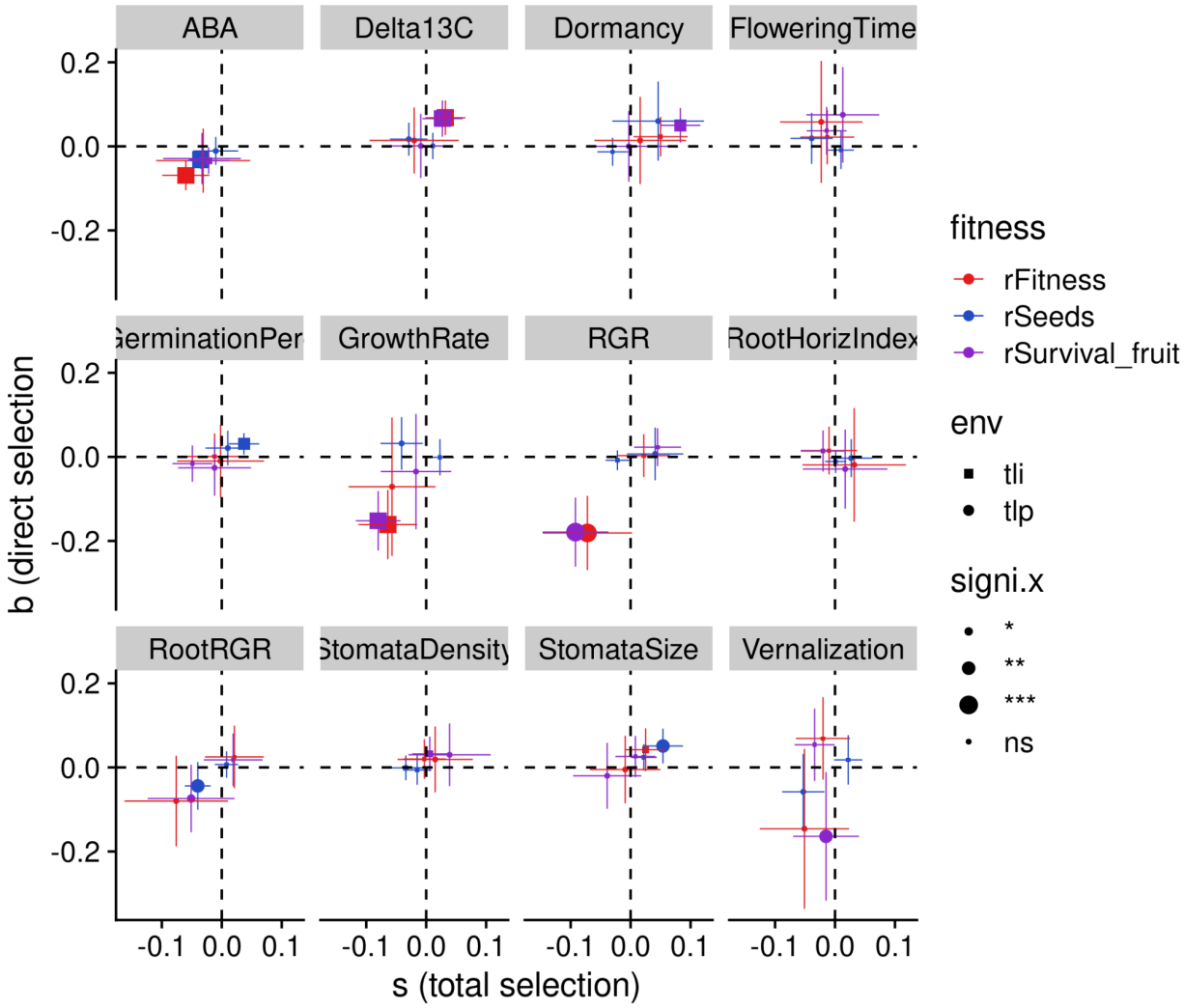

Figure S10. Multivariate selection analysis for 12 focal traits with cool temperature, but low water environment in Tubingen, and high/low planting density fitness data from Exposito-Alonso et al. 2019. Estimates were made from 100 bootstrap samples, establishing the confidence intervals and significance levels; ns= not significant, *=0.05, **=0.01, ***=0.001.

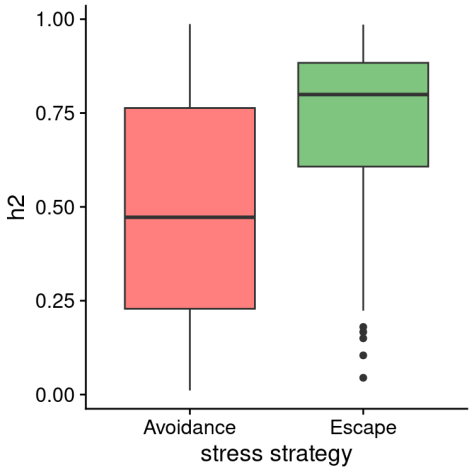

Figure S11. Boxplot of SNP-based heritability estimates for escape traits and avoidance traits post-filtering for traits with inconsistent or low quality heritability estimates; wilcox test p-value=2.6×10^{-8}.

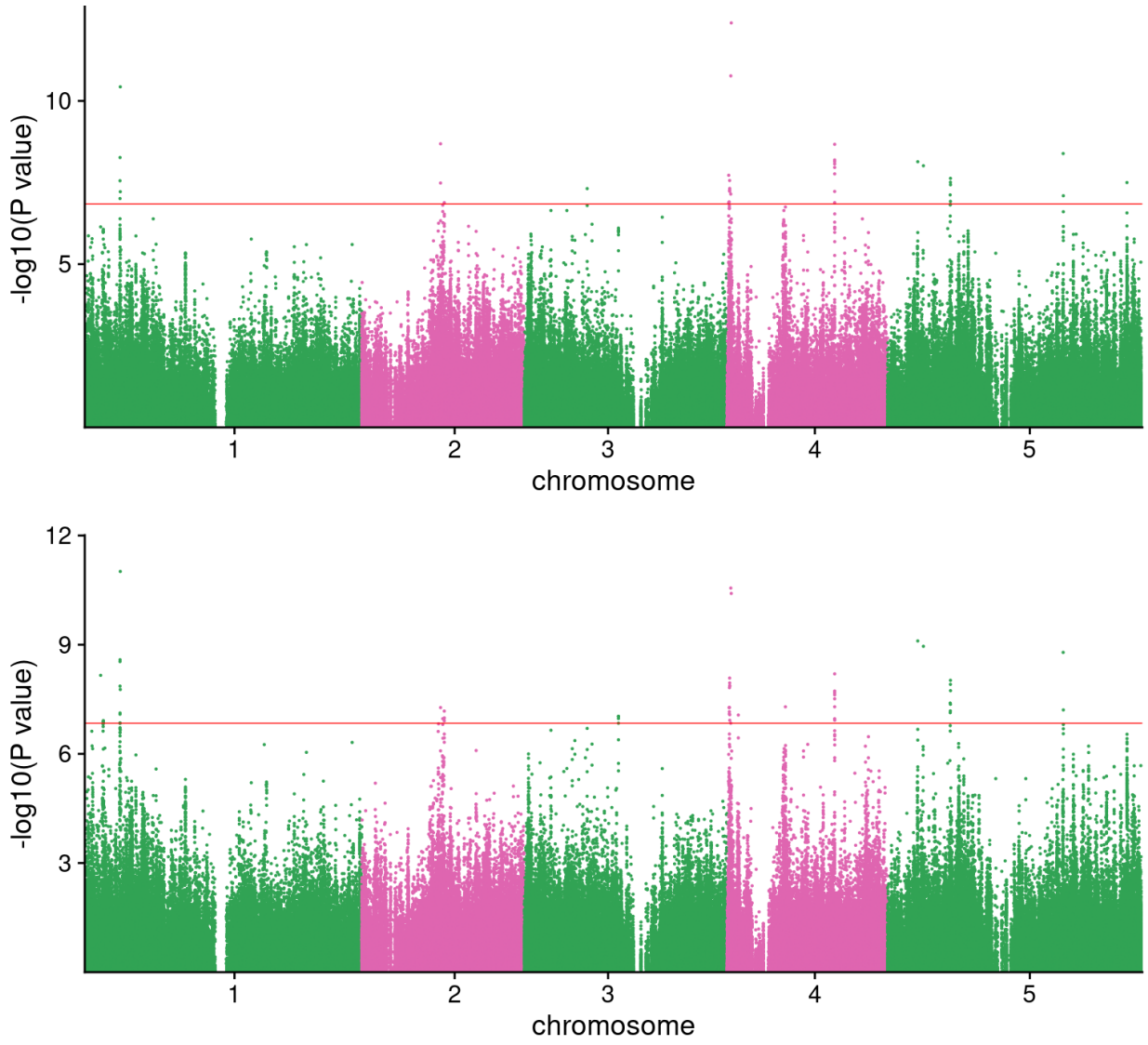

Figure S12. Multivariate GWA between flowering time and growth rate; normalized phenotypic data but not imputed, so the number of overlapping samples, or the total number used in this GWA was 395. Kinship was used to correct for population structure, no genetic PCs (**upper**), with 5 genetic PCs (**lower**).

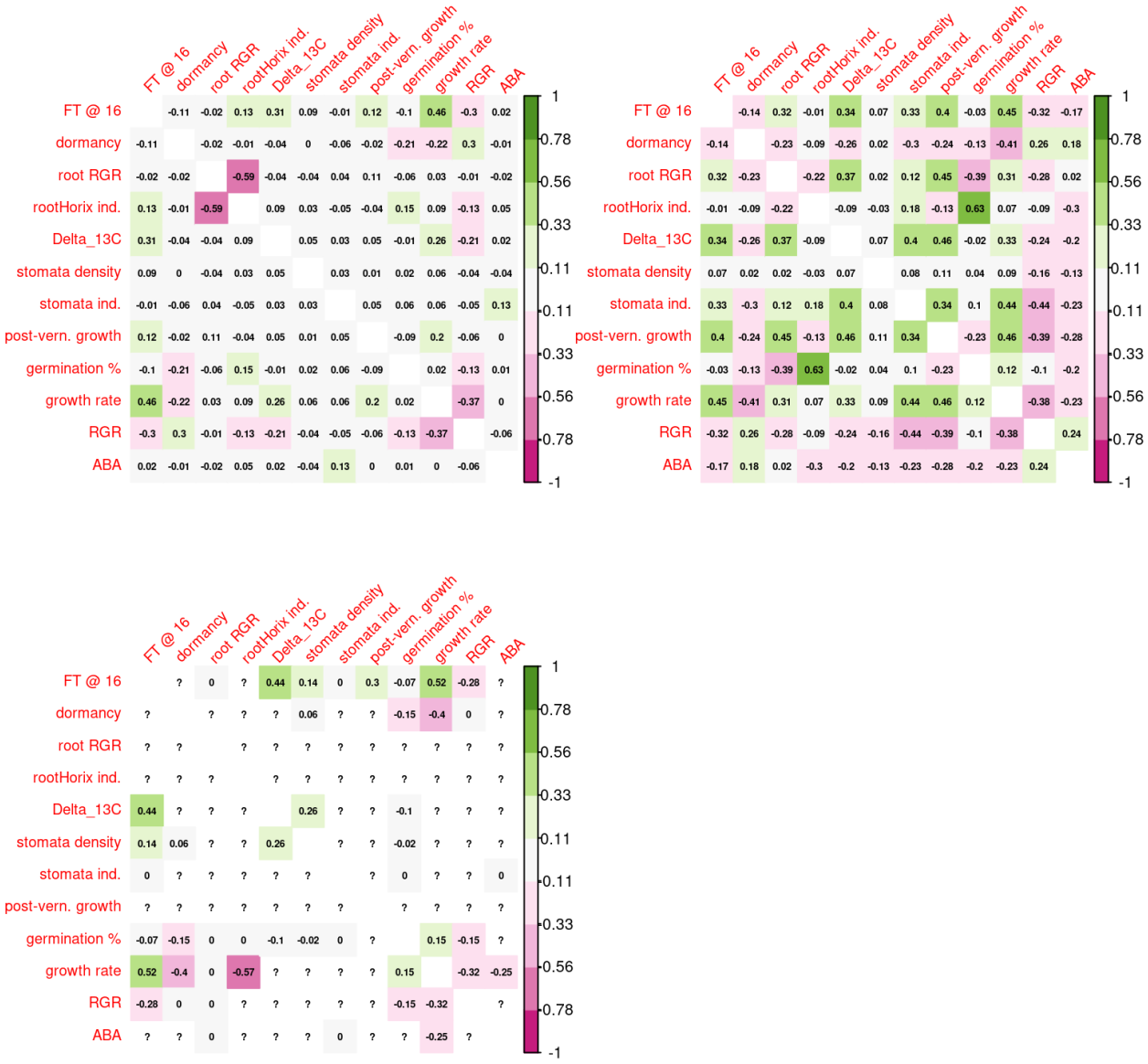

Figure S13. Genetic correlations for target traits estimated through **top left)** summary statistics for SNPs from independent LD blocks, also called an approximate genetic correlation, **top right)** imputed and normalized traits used in multivariate GWAS, and **bottom left)** normalized traits, not imputed, used in multivariate GWAS, in this case many traits did not have enough overlapping samples to perform the method, "?" and "0" indicates not enough data to run the algorithm.

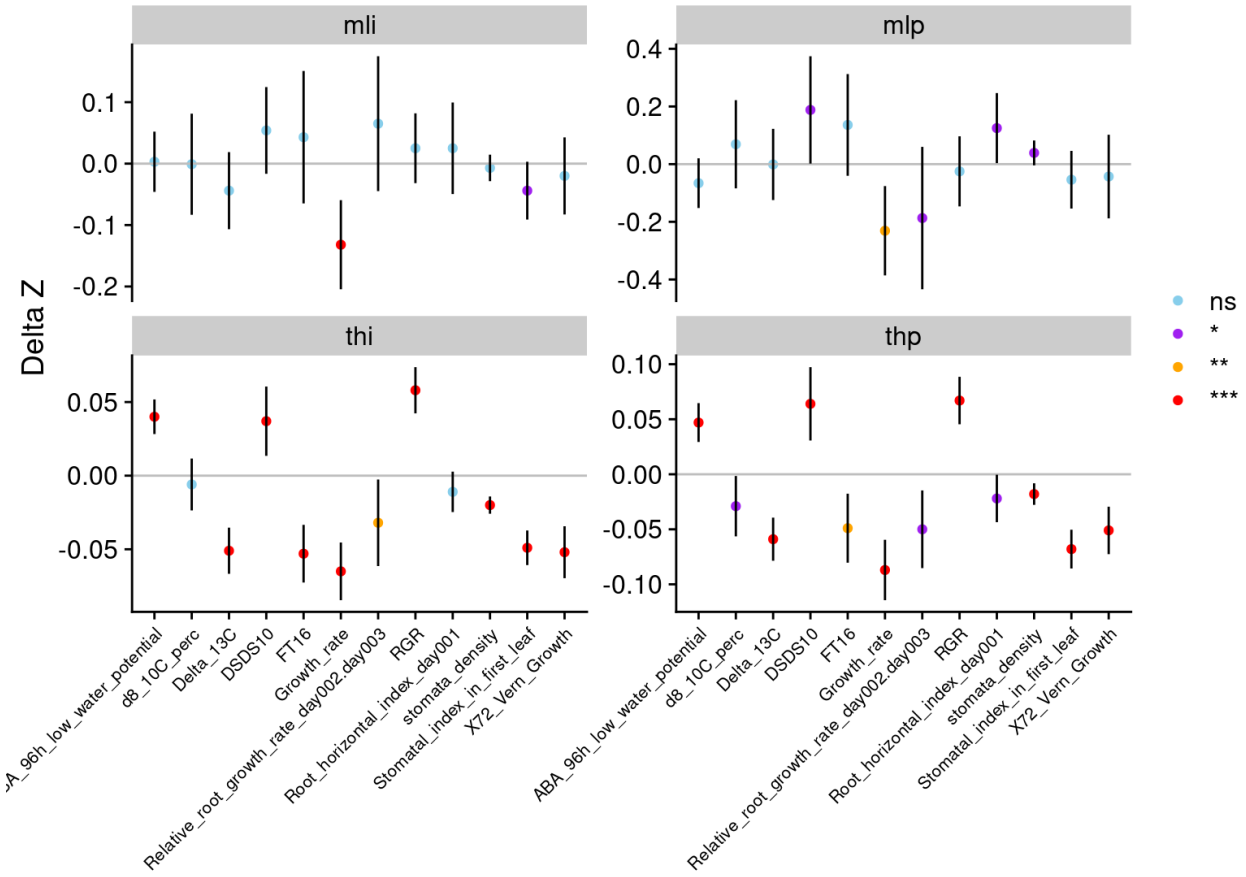

Figure S14. Estimated phenotypic multivariate response to selection, using trait correlations, genetic correlations estimated from multivariate GWA, SNP-based heritability, and total selection coefficients. Estimates were made from 100 bootstrap samples, establishing the confidence intervals and significance levels; ns= not significant, *=0.05, **=0.01, ***=0.001.

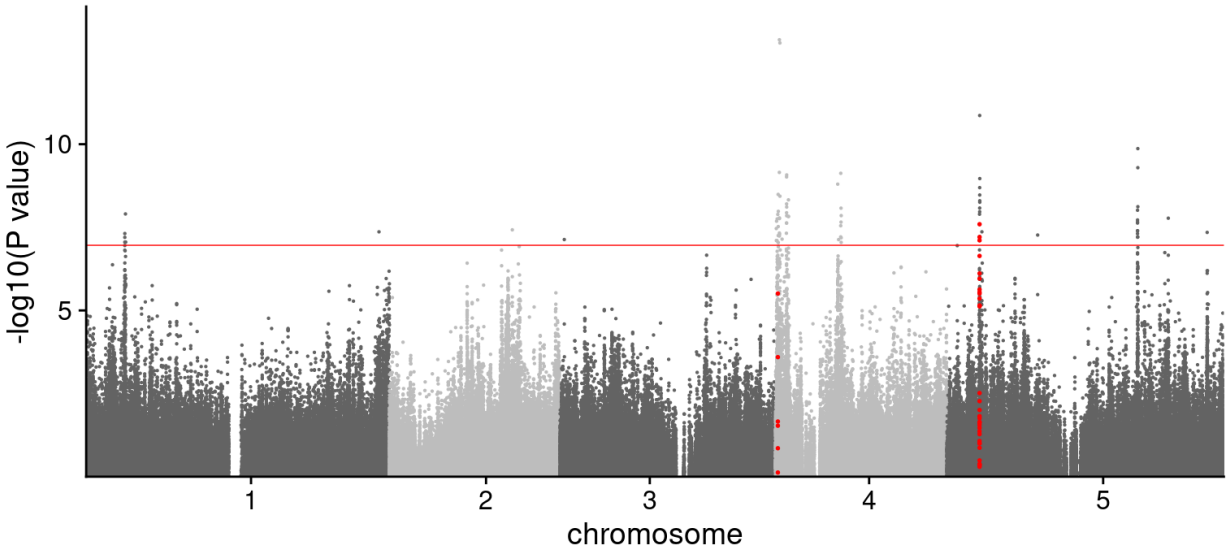

Figure S15. Manhattan plot of multivariate GWA with imputed flowering time and delta_C13 data, corrected for population structure with kinship and 5 genetic pcs; alleles within *Frigida* (chr4) and *Flowering Locus C* (chr5) marked in red.

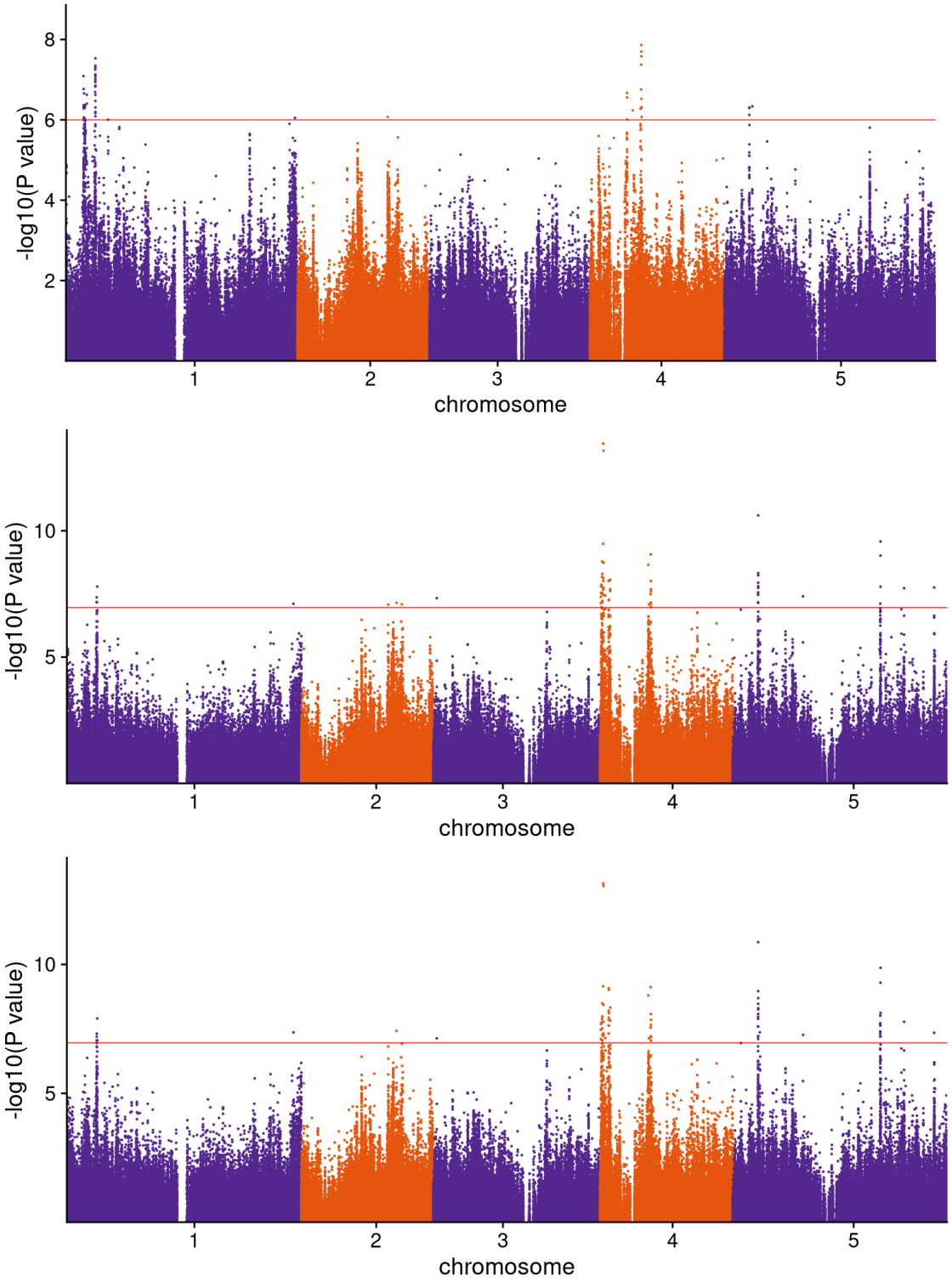

Figure S16. Manhattan plot of multivariate GWA of flowering time and WUE, corrected with kinship, and with **top**) non-imputed trait data and 5 genetic pcs used as covariates in the analysis, **middle**) imputed trait data, no genetic PCS, and **bottom**) imputed trait data and 5 genetic PCs used as covariates. Note the peak on Chr 1 remains significant and narrows as we correct for population structure with 5 pcs, and this more narrow peak includes only 1 gene on chromosome 1, AT1G11540.

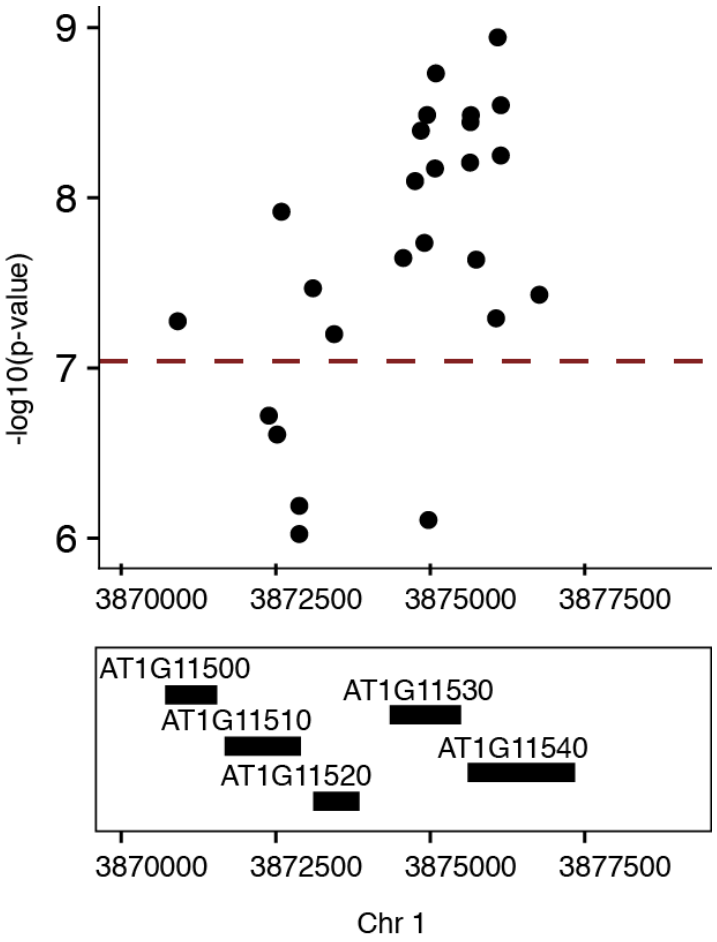

Figure S17. Zoomed in plot of multivariate GWA of flowering time and WUE (**Fig. 3A**) on chromosome 1 showing the high effect peak and the genes within.

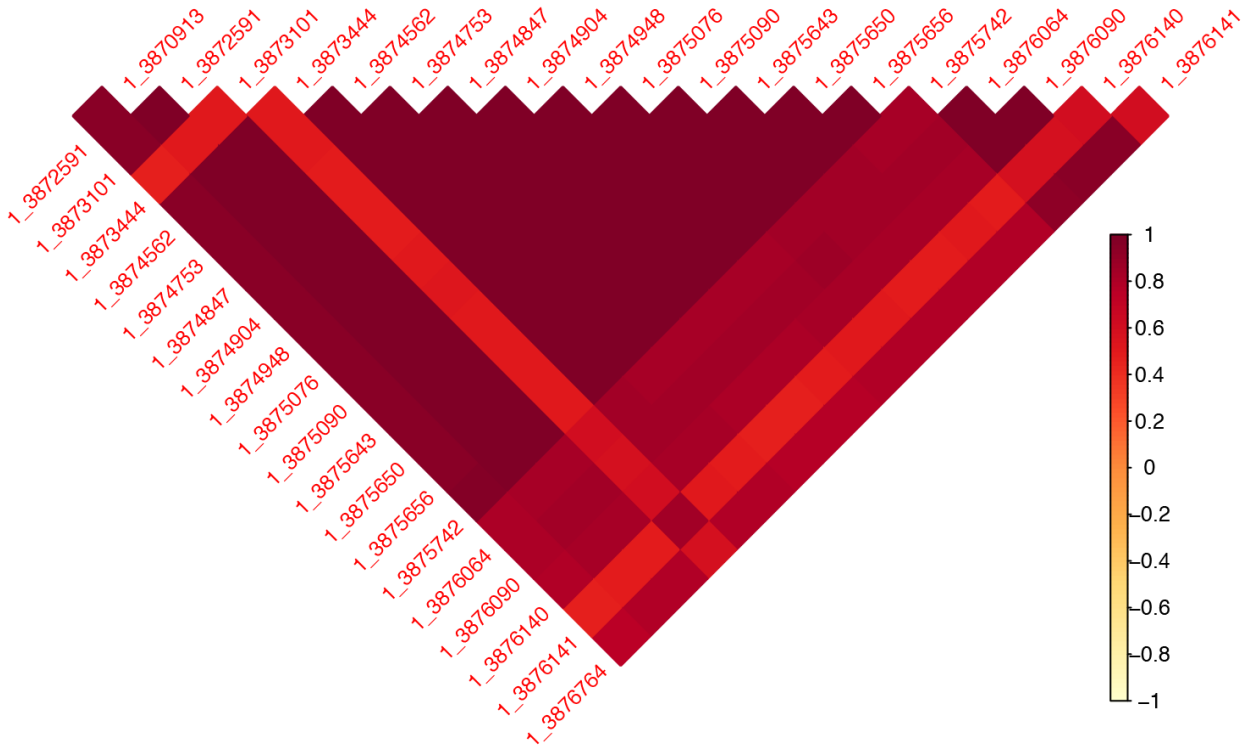

Figure S18. Linkage disequilibrium (r2) estimates amongst the 19 top effect SNPs in the chr 1 high effect peak from Fig. S15.

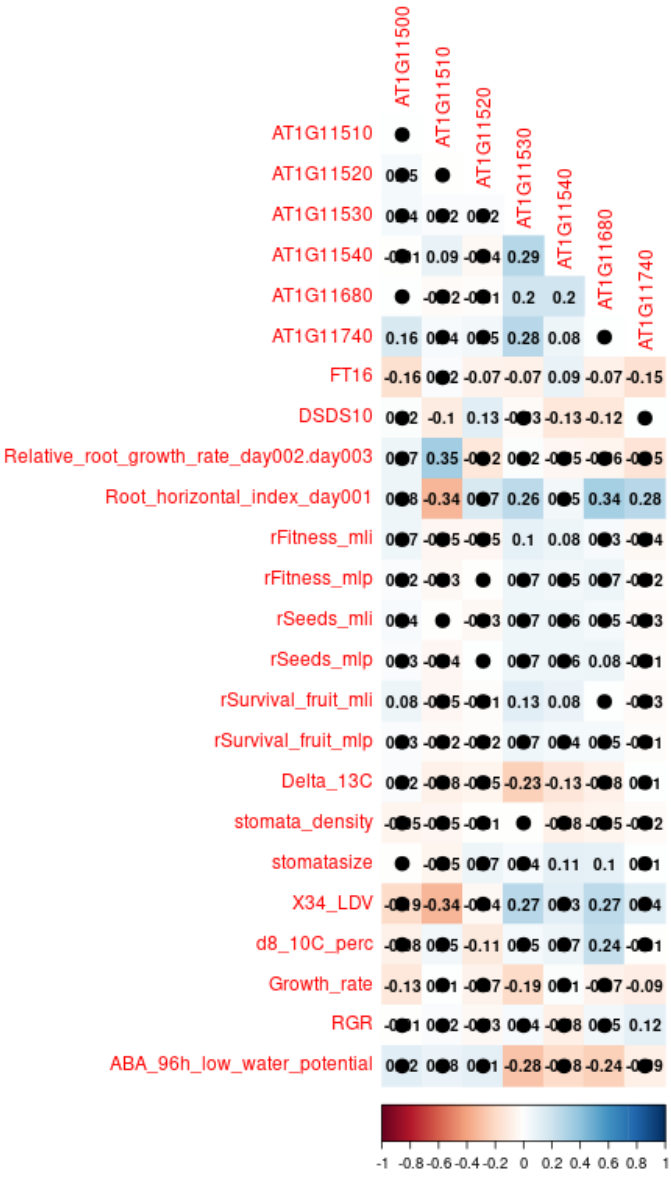

Figure S19. Spearman rank correlations between target traits and the expression of the 5 genes identified in the high effect peak on chromosome 1, cells without a black dot indicated the p-value < 0.2. Expression data are in units of relative transcripts per million.

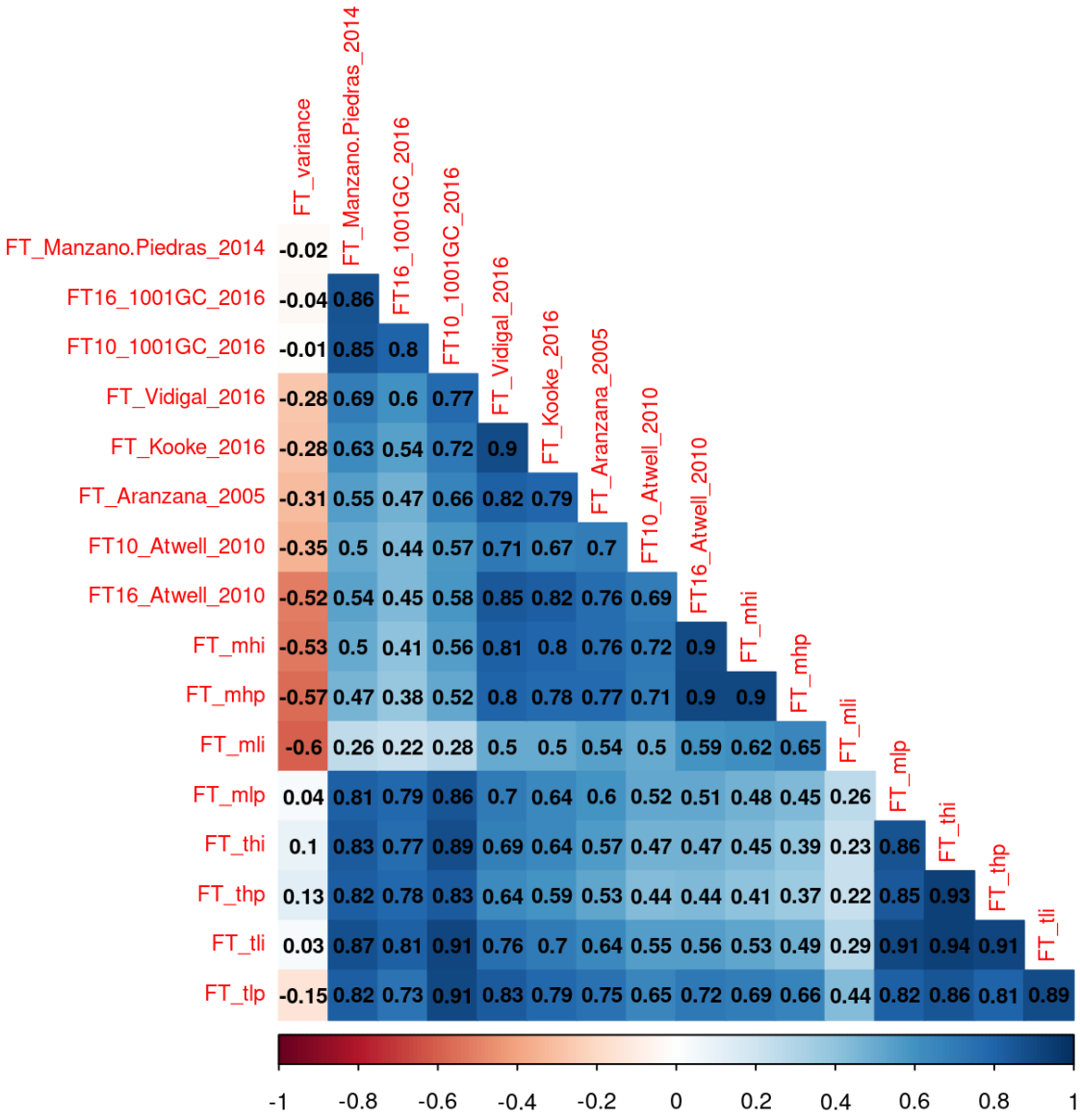

Figure S20. Pearson correlation coefficient estimates of flowering time trait measurements compared across various studies that collected flowering time trait data. The "FT_xxx" traits are from Exposito-Alonso, *et al.* 2019.

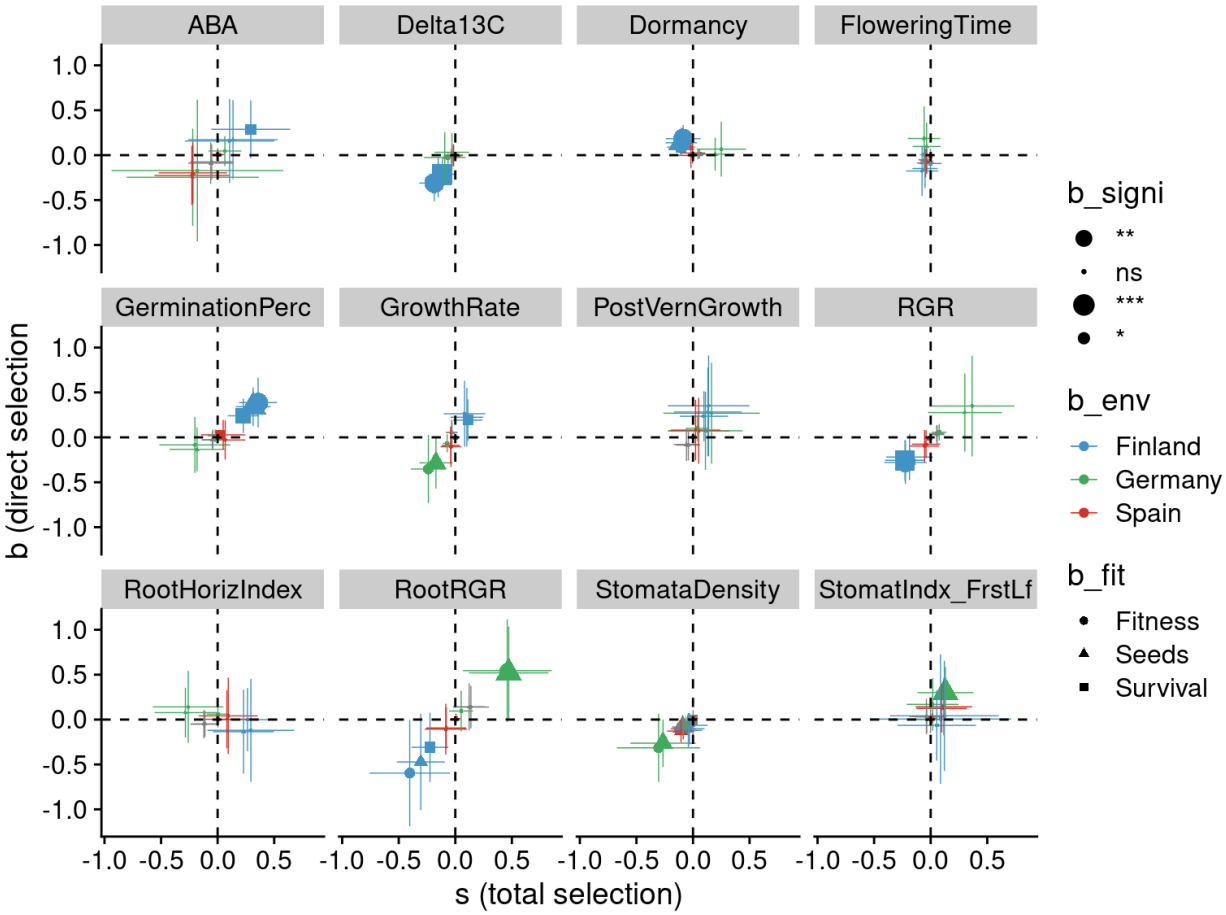

Figure S21. Multivariate selection analysis for 12 focal traits using fitness data from Fournier-Level *et al.* 2011 from 3 locations and 3 different fitness measures. Estimates were made from 100 bootstrap samples, establishing the confidence intervals and significance levels; ns= not significant, *=0.05, **=0.01, ***=0.001.

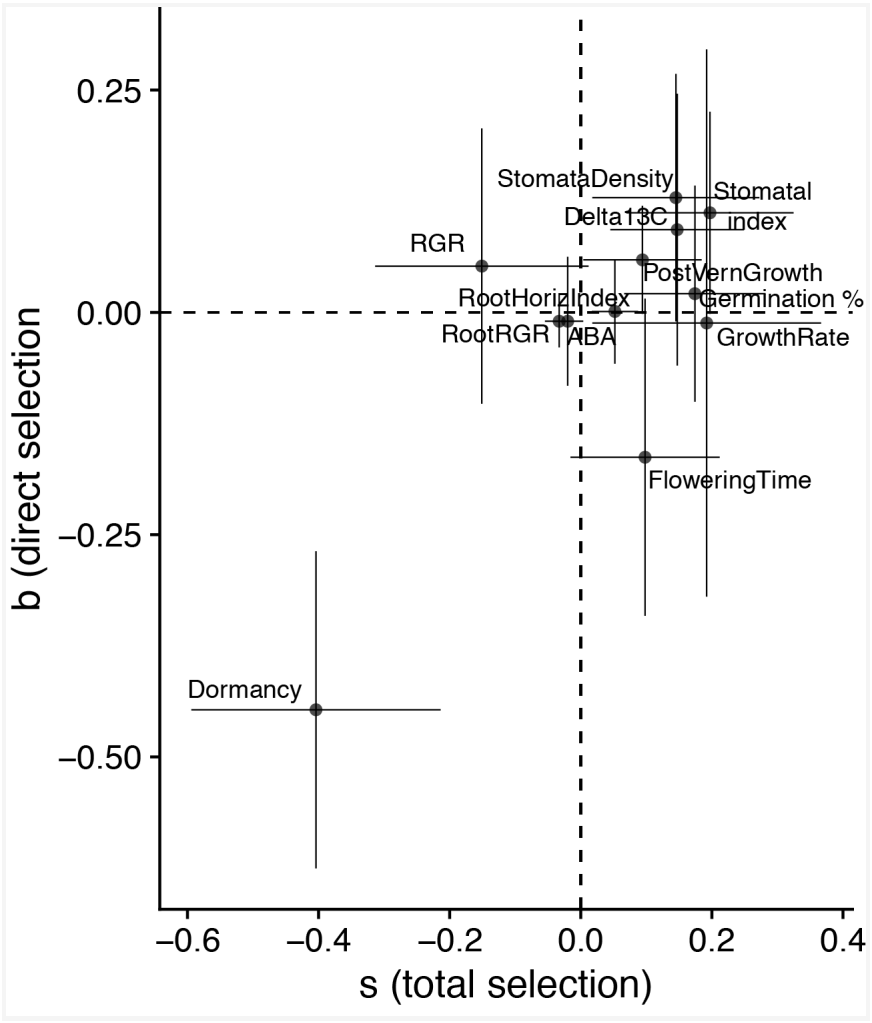

Figure S22. Multivariate selection analysis for 12 focal traits using fitness data from survival data from Manzano-Peidras *et al.* 2014. Estimates were made from 100 bootstrap samples, establishing the confidence intervals and significance levels; ns= not significant, *=0.05, **=0.01, ***=0.001. Interestingly, Manzano-Peidras *et al.* 2014 found evidence for selection for late flowering, but our analysis show that when correcting for correlated traits, there is a negative direct selective effect on flowering time, indicating that in this experiment and in these populations there is also a selection conflict on flowering time.

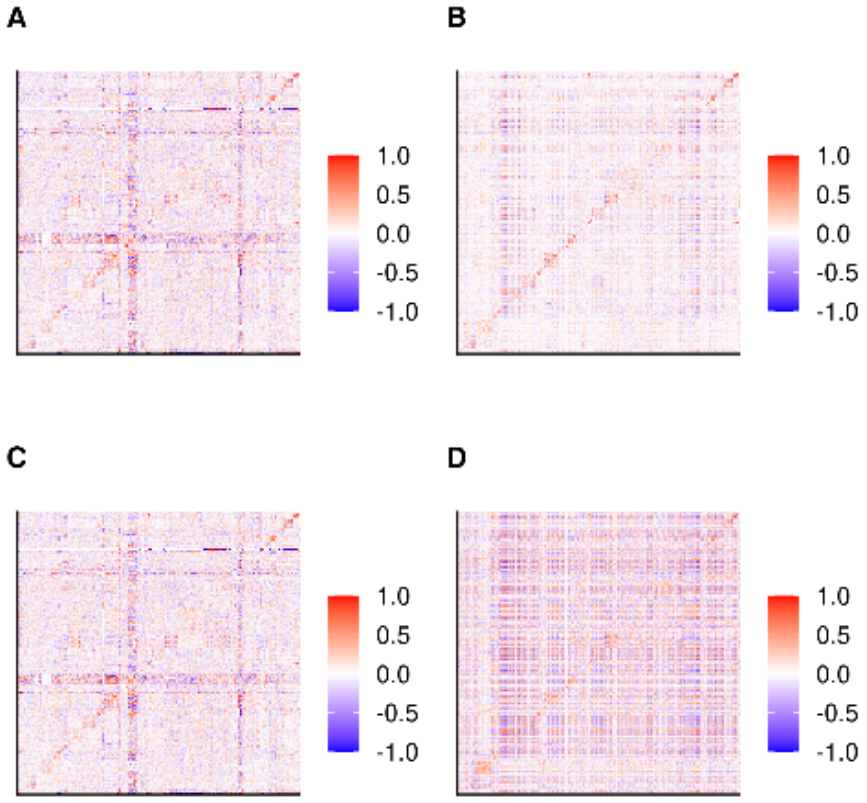

Figure S23. Pearson's correlation coefficients for all phenotypes across various datasets A) raw B) imputed C) raw normalized D) imputed normalized.

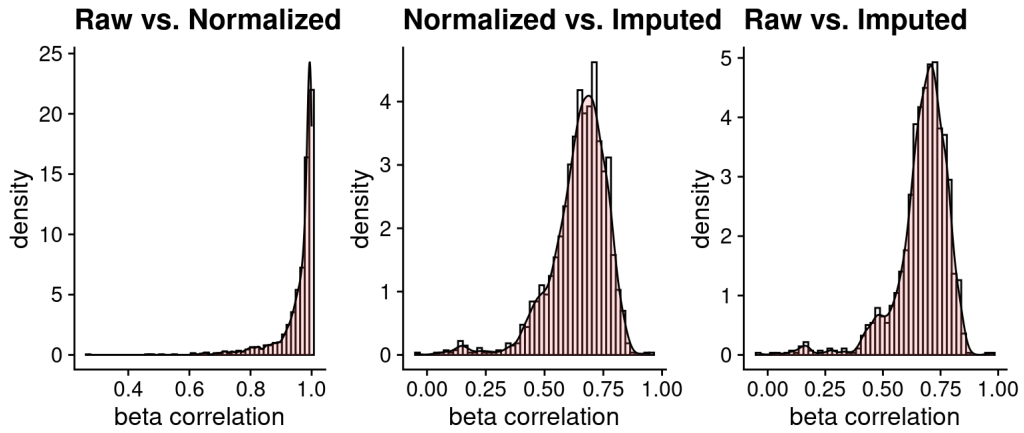

Figure S24. Comparison of Pearson's correlation coefficients for effect size estimates from GWA using raw trait data, normalized data, and imputed data.

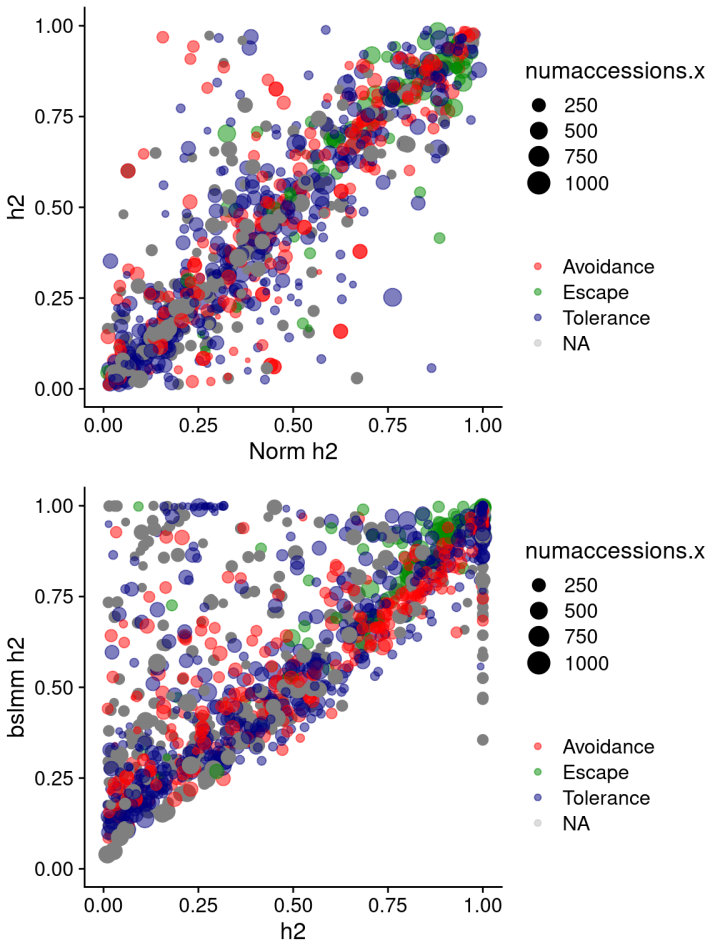

Figure S25. Comparison of SNP-based heritability estimates from normalized and raw phenotype data (top), and from the LMM (with raw data) and BSLMM GWA algorithm (bottom), while removing all estimates where both methods estimated less than 0.01 or greater than 0.99 heritability.

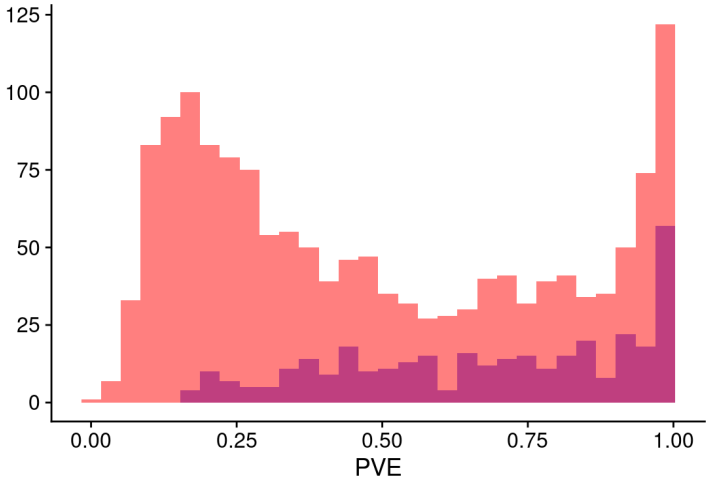

Figure S26. Number of phenotypes with SNP-based heritability estimates within 0.15 difference of each other across estimations (red) compared to phenotypes with a greater than 0.15 difference across estimation techniques (purple).

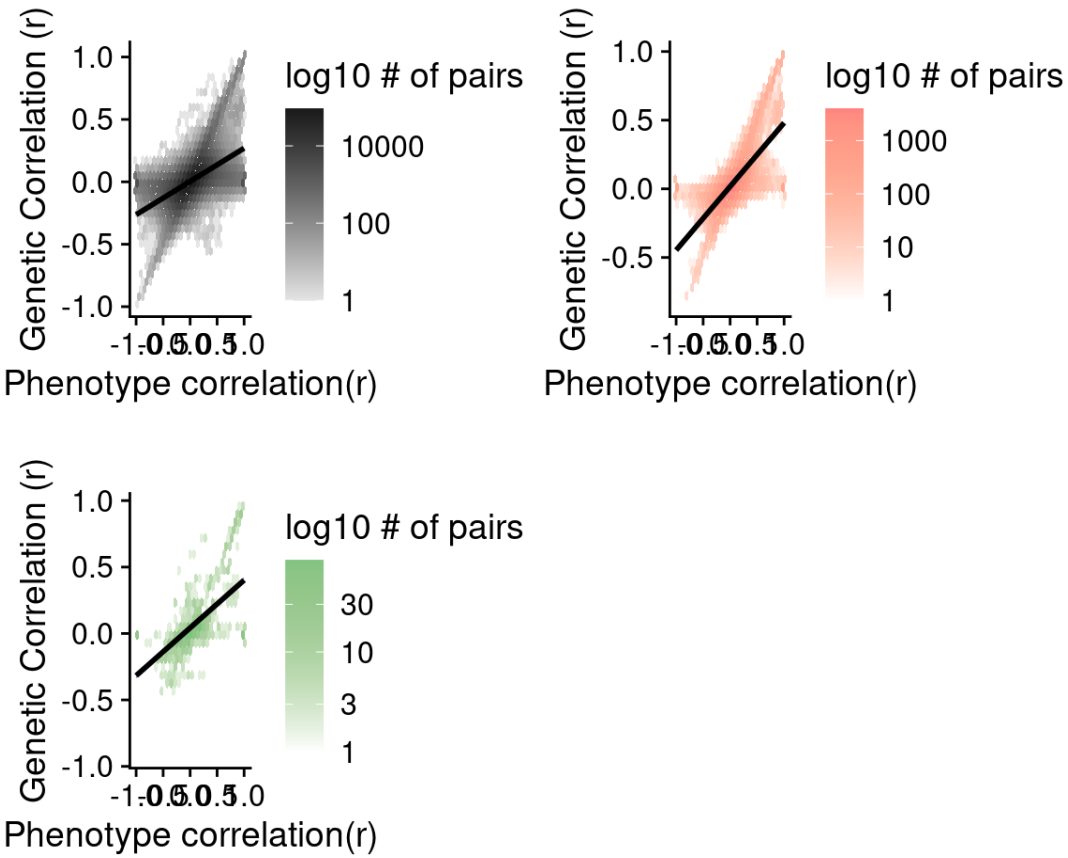

Figure S27. Genetic correlations compared to trait correlations between all pairs of traits (top-left, black), only avoidance classified traits (top-right, pink), and only escape classified traits (bottom-left, green)

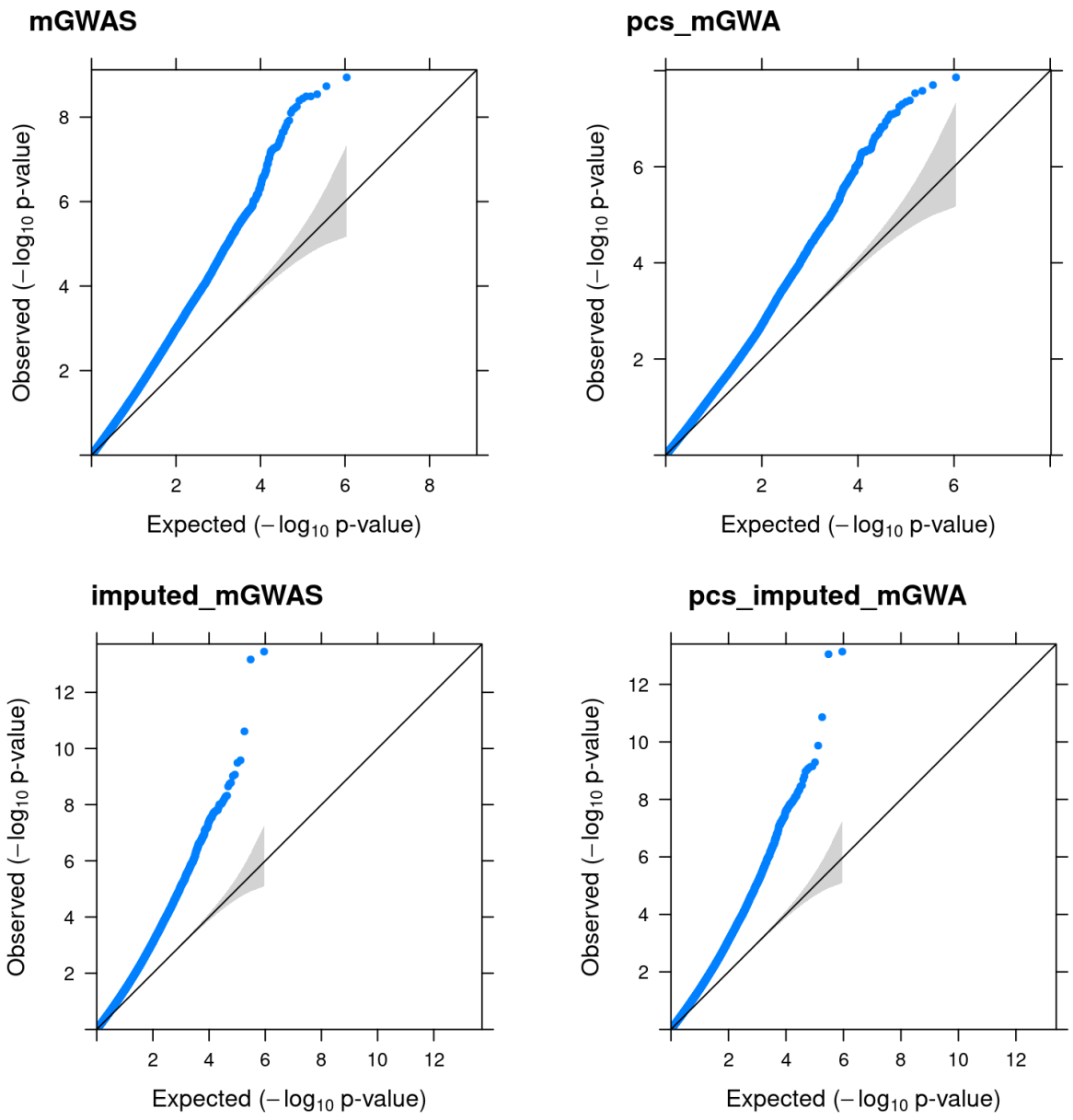

Figure S28. QQplots for multivariate GWAS with flowering time and WUE trait data for different GWAs run with just the 248 samples that overlapped (top left), with 5 genetic PCs (top right), and imputed trait data so all 1,135 samples (bottom left), also with 5 genetic PCs (bottom right).